The human respiratory system

Anders Ström

April 28, 2014

Project in Computational Science: Report

Abstract

A model of the human respiratory system containing the diaphragm and the lower six ribs is created from a commercial model. The diaphragm is modelled by a mass spring system and the ribs are moved rigidly using affine transformations. The ribcage is attached to the diaphragm based on proximity using ray triangle intersection. The action line method for modelling muscle contraction is implemented and tested. Stable contraction of the diaphragm is achieved but relaxation of the diaphragm during expiration shows some instabilities and the diaphragm does not return to its original position.

Contents

1 Introduction

1.1 Background

Mechanical ventilation is frequently used in intensive care units to treat patients suffering from respiratory failure and other critical illnesses. Although mechanical ventilation is life saving it can also cause complications in the patient's health condition. Ventilator-induced diaphragmatic dysfunction (VIDD) is a term referring to the loss of diaphragm function and structure due to mechanical respiration. This decrease in functionality and loss of structure complicates the weaning from the mechanical ventilator [11], increasing morbidity and mortality rates, and in extension the cost of care. A clinical review of the occurrence of VIDD in human patients has been made by Jaber et al. in [6].

The ability to study the effect of mechanical ventilation in human patients is limited due to ethical reasons, instead animal trials are performed. The **3Rs** principle is an ethical guideline for finding alternatives to animal studies. The **3Rs** refers to *replacement*, *refinement*, *reduction* [2]. In the long term, a computer simulation of the human respiratory system could serve as a replacement of animal studies.

1.2 The Human Respiratory System

Physiological respiration, which is the term for breathing naturally, is performed by using the respiratory muscles to increase and decrease the volume of the thoracic cavity. This changes the air pressure in the lungs and allows air to flow in and out through the airways.

The most important muscle of inspiration is the diaphragm. The diaphragm is a thin dome shaped sheet of muscle which separates the thoracic and abdominal cavity. It is attached to the lower six ribs, the xiphoid of the sternum and the lumbar vertebrae. During inspiration it contracts and moves down to increase the vertical dimension of the thorax. Also the ribcage is expanded up and out which increases the lateral and anteroposterior dimensions of the thorax. The outward expansion of the ribcage is initiated by the contraction of the external intercostal muscles which attach adjacent ribs from the lower border of one rib to the upper border of the rib below. The expansion of the ribcage is a complicated process also involving both the diaphragm and the abdominal compartment.

Expiration is passive during quiet breathing and is performed by the elastic recoil of the lungs and chest wall to their equilibrium positions. Air pressure in the lungs is then increased, causing air to flow out of the lungs. During heavy breathing, which occurs during exercise or in case Chronic Obstructive Pulmonary Diseases (COPDs), expiration is active. The main muscles of expiration are those of the abdominal wall. During inspiration the abdominal wall is pushed out by the descending of the diaphragm. Contraction in the abdominal muscles increases the pressure in the abdominal cavity and pushes the diaphragm upwards. The internal intercostal muscles also help to perform active expiration by pulling the ribcage downward and inward, thereby working in the opposite manner of the external intercostal muscles.

1.3 Aim

The aim of the project is to improve an existing model of the human respiratory system with focus on a better geometric description of the diaphragmatic zone of apposition and to simulate muscle contraction in the diaphragm.

In the long term the goal is to be able to simulate the effects of mechanical ventilation on the respiratory muscles and to improve intensive care with respect to VIDD.

2 Methods

This project is based on previous work where a simulation of the diaphragm was implemented in Matlab [10]. Implementations are made as extensions of the existing simulator.

2.1 3d Model

A commercially available three-dimensional (3d) model from Anatomography[1] is used . The parts used are listed below and figure 1 shows the complete model.

- diaphragm
- 7-12 ribs
- 7-10 costal cartilage
- 7-12 thoracic vertebrae

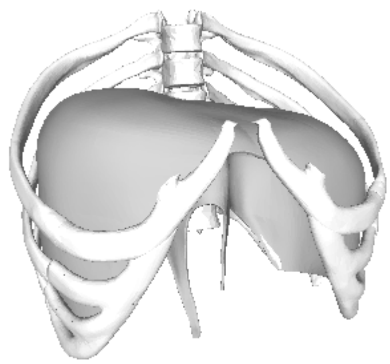

Figure 1: The original geometry of diaphragm, 7-12th ribs and vertebrae, 7-10 costal cartilages

Each of the components are individual surface enclosed volumes represented by a set of vertices, which are points in space, and a set of triangular faces defined by three corner vertices. The top and bottom layers of the diaphragm are separated and the openings for the vena cava and aortic hiatus are closed.

The diaphragm is then re-meshed using the *remeshsurf* function of the iso2mesh [5] toolbox for Matlab. A software called meshlab [13] is used to manually edit the mesh and to down sample the model of the skeletal parts.

2.2 Ribcage Kinematics

Movement of an individual rib during ventilation can be described as a combination of a bucket- and pump handle [7]. The ribs are treated as rigid and the costal cartilages are treated as rigid extensions of the ribs. The bucket handle motion is performed as rotation around the *y-axis* and the pump handle motion as rotation around the *z-axis* around the ribs attachment in the spine. This is shown in Figure 2 for the left seventh rib.

The affine transformations of the ribs are performed with a 4×4 transformation matrix. The rotation-only transformation matrix has the following form,

$$\begin{pmatrix} x_{t+1} \\ y_{t+1} \\ z_{t+1} \\ 1 \end{pmatrix} = \begin{pmatrix} R_{11} & R_{12} & R_{13} & 0 \\ R_{21} & R_{22} & R_{23} & 0 \\ R_{31} & R_{32} & R_{33} & 0 \\ 0 & 0 & 0 & 1 \end{pmatrix} \begin{pmatrix} x_t \\ y_t \\ z_t \\ 1 \end{pmatrix} \tag{1}$$

and the translation-only matrix,

$$\begin{pmatrix} x_{t+1} \\ y_{t+1} \\ z_{t+1} \\ 1 \end{pmatrix} = \begin{pmatrix} 1 & 0 & 0 & T_x \\ 0 & 1 & 0 & T_y \\ 0 & 0 & 1 & T_z \\ 0 & 0 & 0 & 1 \end{pmatrix} \begin{pmatrix} x_t \\ y_t \\ z_t \\ 1 \end{pmatrix} \tag{2}$$

These can be combined to perform rotation and translation with one matrix vector multiplication. The rotation-only matrix performs rotation around the origin, so to rotate a rib around its rotation point it is first translated such that the rotation point is at the origin, rotation is then performed and then the rib is translated back so the rotation point is in its original position. The rotation points for each rib are chosen from the extreme lateral points in the corresponding vertebra, i.e. the left seventh rib rotates around the left most point of the seventh vertebra.

2.3 The Diaphragm

The diaphragm is treated as consisting of three different types of tissue. The top part shown in figure 3 is called the central tendon and is a rigid mix of tendon and muscle tissue and does not contract during respiration. The attachments to the ribcage are moved along with the ribs and the attachment to the spine are stationary. Between the central tendon and the rigid attachment is the zone of apposition (ZAP). This is the muscular part where contraction occurs.

The two layers of the diaphragm are connected with a ray triangle intersection method. This is done by following the normal direction of the vertices in the bottom layer of the diaphragm and checking for intersection with the faces in the top layer. If an intersection occurs a connection is made between the bottom vertex and the three corner vertices in the face of the top layer. Since the

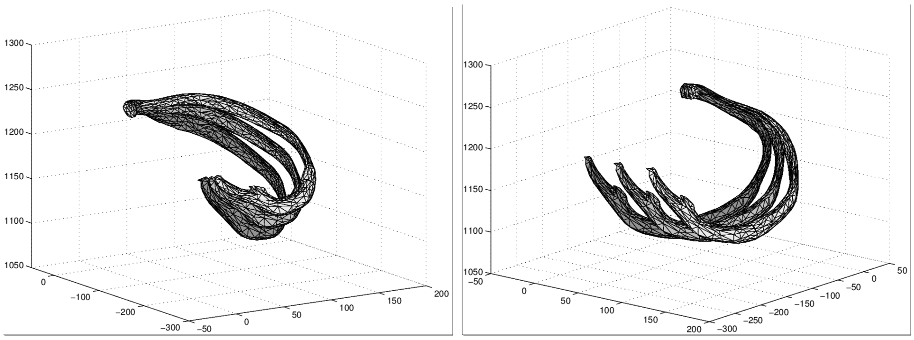

(a) bucket handle, rotation around y-axis (b) pump handle, rotation around z-axis

Figure 2: pump- and bucket handle motion of the left seventh rib at the beginning of and end of inspiration as well as one intermediate position. The motion is exaggerated

diaphragm is not a convex surface a maximum distance parameter is used to avoid undesirable connections. The method used was implemented in [10] and is based on a method suggested by Möller and Trumbore [8]. The two connected layers helps give the model some rigidity and it also gives the diaphragm model a physical thickness. The bottom layer represents the part of the diaphragm that faces the abdominal compartment and the top layer the part facing the thoracic cavity.

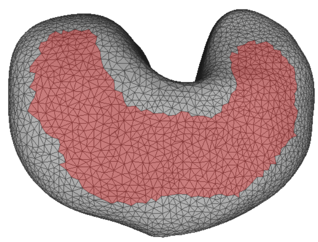

Figure 3: Top view of the diaphragm with the central tendon marked in red.

2.3.1 The Mathematical Model

The mathematical model used for the diaphragm was developed by Nilson in [10], where a full analysis can be found, on which the following section is based.

The diaphragm is described with a mass-spring model (MSM). Each vertex x_i in the mesh is represented by a mass m_i and the mesh edges between two vertices (as well as connections between the layers), x_i, x_j are defined as springs with a spring-constant k_{ij} and a resting length $L_{0,ij}$. The second position derivative for x_i can be obtained at each time-step as

$$\frac{d^2x_i}{dt^2} = m_i^{-1} \cdot \underbrace{(F_i^{ext} - F_i^{int} - F_i^v)}_{\text{F}} \tag{3}$$

where the F_i^{ext} is an external force placed on the vertex, F^{int} is the internal force resulting from the springs acting on the mass,

$$F_i^{int} = \sum_{j \in M(i)} k_{ij} * (L_{t,ij} - L_{0,ij}) \cdot \frac{x_i - x_j}{L_{t,ij}} \tag{4}$$

where $M(i)$ is a list of vertices connected to x_i with a spring and $L_{t,ij}$ is the current distance between vertices x_i, x_j. The term F_i^v is viscous damping,

$$F_i^v = \sum_{j \in M(i)} \gamma_{ij} \frac{d(x_i - x_j)}{dt} \tag{5}$$

The equations of motion for the MSM are integrated in time using Verlet integration [4]. The position is obtained from,

$$x^{n+1} = 2x^n - x^{n-1} + \Delta t^2 m^{-1} F + O(\Delta t^4) \tag{6}$$

and the velocity, which is needed in the system for calculating the damping can be defined as

$$v^{n+1} = \frac{x^{n+1} - x^{n-1}}{2\Delta t} + O(\Delta t^2) \tag{7}$$

The choice of integrator is discussed thoroughly in [10] and is made with respect to stability and efficiency.

To avoid unnatural stretching of the springs and to introduce rigidity a constrained distance method (CDM) is used to relax the mass-spring system. This technique is commonly used to simulate cloth. The relaxation is applied after the equations of motion have been solved and works by simply moving a pair of connected vertices x_i, x_j, together such that the distance between them equals the spring resting length $L_{0,ij}$ and at the same time maintaining the direction of the spring. The CDM is iterative so for a vertex that is subject to n relaxations the CDM is applied n times to all springs attached to it. The CDM can be applied locally to specific vertices which can be used in the diaphragm to capture the different properties of the central tendon and ZAP.

2.3.2 action lines

Nedel and Thalman [9] use a concept called action lines to model muscle contraction in spindle-shaped mass-spring muscles, such as the Biceps Brachii. The action line defines the direction of the contracting muscle action as one or more straight lines between the insertion- and origin points of the muscle. An action line can be separated with a guide point such that it does not e.g. pass through bones or joints. This has been used previously to model muscle contraction in the diaphragm by Villard et. al[12].

The diaphragm does not have discrete origins and insertions. The insertion of the diaphragm is along the edge of the central tendon and the origin is along the lower six ribs, spine and xiphoid. The action lines are represented by thin segments in the muscular part of the diaphragm as can be seen in Figure 4a. All vertices in the muscular part of the diaphragm are assigned to the closest action line and the force direction is treated as piecewise constant. The diaphragm is curved so a number of equidistant guide points can be used to make the direction of the action line closer to the tangential surface of the diaphragm. Figure 4b shows the separation of the vertices to the action lines with two guide points used.

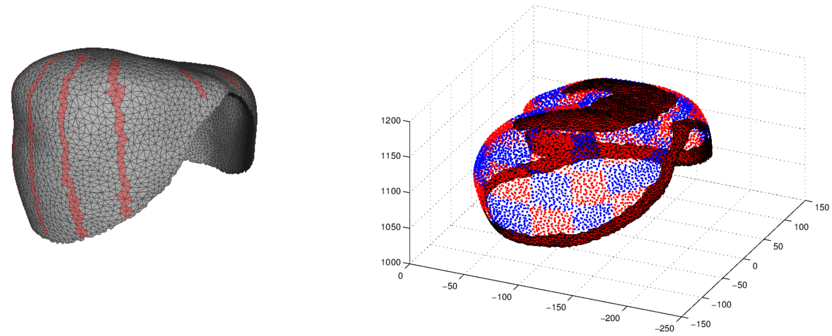

(a) Segments used for defining the contracting forces with action lines.

(b) piecewise interpolation of muscle force direction using two guide points

Figure 4

2.4 Attaching the Diaphragm to the Ribcage

The diaphragm is attached to the lower six ribs. Vertices in the diaphragm are attached to the ribcage based on proximity using the same ray triangle intersection method used for connecting the diaphragm layers. Each vertex in the top layer of the diaphragm is tested for attachment by following the normal direction and checking for intersection with any face in the ribcage. If an intersection occurs and the distance to the intersection point is smaller than a predefined minimum distance, d_{min}, an attachment is made with the corresponding rib.

2.5 Abdominal Compartment

During inspiration, as the diaphragm descends, the abdominal wall is displaced forward. This leads to increasing pressure in the abdominal compartment during inspiration. The Abdominal pressure does not only depend on thoracic volume, e.g body posture and contraction of the abdominal muscles also effects it. Measurements of the relation between thoracic volume and abdominal pressure can be made on subjects that are stationary [3].

The abdominal pressure is modelled via the sum of external forces acting in the outward pointing normal direction on the vertices in the diaphragm. The magnitude of the force is treated as linear with respect to the change in thoracic volume. The change in thoracic volume is approximated from the outward rotation of the ribcage and the mean vertical position of the vertices in the central tendon.

3 Result and Discussion

A model is created with the diaphragm and lower ribcage as shown in Figure 5. The diaphragm has 10907 vertices and 21131 faces and the model of the ribcage has a total of 5643 vertices and 11199 faces. The maximum rotation angle for each rib corresponding to bucket and pump handle movement can be set individually.

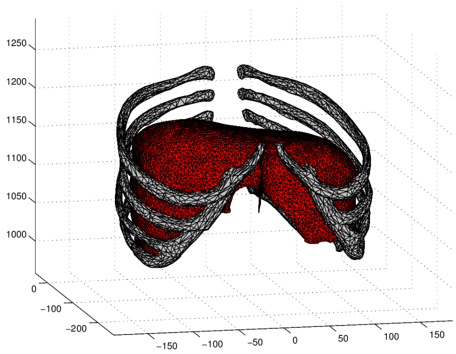

Figure 5: Model of the respiratory system containing the diaphragm and the lower six ribs

3.1 Abdominal Compartment

Calculating the normal directions of the vertices in each time step ads a lot of work, thus slowing down the simulation. The vertex normals are therefore treated as constant during the simulation. This affects the shape of the diaphragm during simulation but the main contribution of the abdominal forces is that it gives support and prevents the diaphragm from folding as well as aiding the recoil of the diaphragm during expiration.

3.2 Ribcage Attachments

The attached nodes are rotated rigidly along with the corresponding rib. A problem encountered with the model is that parts of the ribcage intersect the mesh of the diaphragm in areas where attachments would be made. Currently this is worked around by rotating the ribcage slightly outwards before applying the attachments. Figure 6 shows the attached nodes for different values of the maximum distance parameter d_{min}.

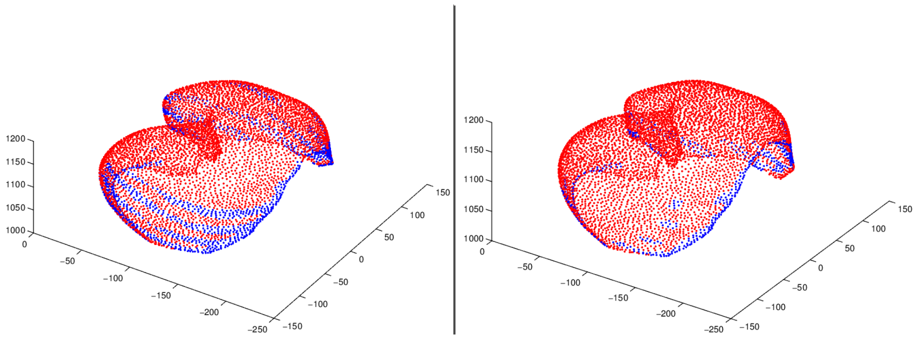

(a) $d_{min} = 10$ (b) $d_{min} = 5$

Figure 6: Blue areas represent vertices in the diaphragm attached to the ribcage.

3.3 Simulating Muscle Contraction

To test the proposed method for achieving muscle contraction a separate model is used which does not include the ribcage and is stationary along the entire lower boundary. The initial idea is to apply external forces on the masses in the zone of apposition. This however leads to folding of the diaphragm. The folding result becomes apparent when considering that the relaxed mass spring system used originates from cloth simulation. A comparison would be to imagine the folding which would occur when trying to push a table cloth together. Using the abdominal pressure to prevent folding is proven not to be possible. The pressure has to be too large and thereby counteracts the contracting forces almost completely. Too large pressure also blows up the diaphragm in a balloon like manner. This effect can be counteracted by using the relaxations in the zone of apposition but this also counteract any contraction.

Another approach is to change the spring resting length with respect to the direction of the action line. The contractions can then be simulated as a periodic function

$$L_{n,ij} = \|E_{0,ij} - s \cdot \frac{1}{2}(1 - cos(2\pi \frac{t}{T})) \cdot (E_{0,ij} \cdot f)f\|_2 \tag{8}$$

where $E_{0,ij}$ is the edge in vector form corresponding to the spring at the start of the simulation, f is the direction defined by the action line and $0 < s < 1$ defines the maximum amount of contraction at the end of inspiration. Stable contraction of the diaphragm is accomplished in this manner. Figure 7 shows the diaphragm at the beginning and end of inspiration. However, relaxing the diaphragm during expiration leads to unstable behaviour and the diaphragm does not relax back to its initial state. This behaviour is present even for very small contractions.

4 Conclusions

The suggested method for simulating muscle contraction does not yield a realistic result of the full ventilation cycle. The model is limited and further physiological components could be added e.g. the lungs and a full ribcage. Another possible

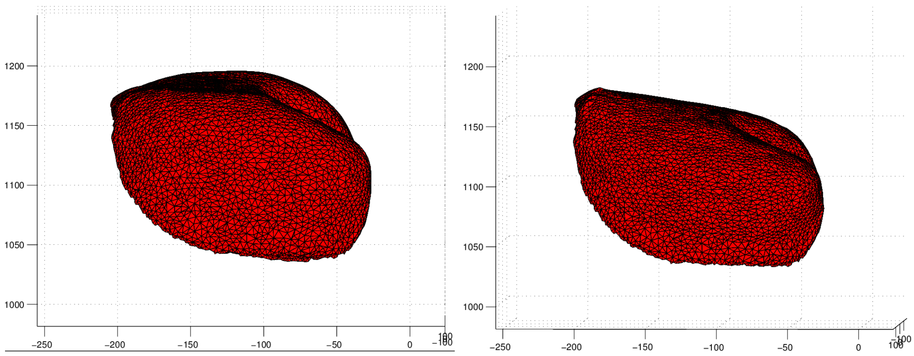

(a) relaxed (b) contracted

Figure 7: Diaphragm at the beginning and end of inspiration with maximum contraction defined by $s = 0.3$

extension would be to add conditions preventing the diaphragm from exceeding the inner dimension of the thoracic cavity. The parameters specifying the movement of the ribcage and the diaphragm-ribcage attachments needs to be tuned and validated with clinical data. What is lacking in the current model is that it does not allow simulation of muscle contraction. This would be a good focus of attention in future development which may include changing the mathematical description of the diaphragm as well as the approach for representing contractions.

Acknowledgements

Thanks to my supervisors Nicola Cacciani, MD specialist at the neurosciences department, and Elisabeth Larsson, senior lecturer at the department of information technology, for valuable input throughout the project.

References

[1] bodyparts3D. The database center for life science licensed under cc attribution-share alike 2.1 Japan, 2013.

[2] Karl-Johan Börjesson (2009). *3Rs - an important ethical principle* Available: http://www.djurforsok.info/english/home/ethics/the3rsanimportantethicalprinciple.4.1c39844f11d7804ba518000586.html

[3] E. D'Angelo, J. Milic-Emili. 2005 BC Decker Inc, *Physiologic Basis of Respiratory Disease,* Chapter 2.

[4] Ernst Hairer, Christian Lubich, Gerhard Wanner. *Geometric numerical integration illustrated by the Strömmer/Verlet method.* 2003, Acta Numerica, volume 12, p. 399-450.

[5] iso2mesh, License: GPL v2 or later. Available: http://iso2mesh.sourceforge.net/

[6] Jaber S, Jung B, Matecki S, Petrof BJ. *Clinical review: ventilator-induced diaphragmatic dysfunction–human studies confirm animal model findings!* Crit Care. 2011 Mar 11;15(2):206. doi: 10.1186/cc10023.

[7] Peter T. Macklem & Jere Mead, editors. *Handbook of Physiology: Section 3: The Respiratory System*, volume III, Part 1 & 2

[8] Tomas Möller and Ben Trumbore, *Fast, minimum storage ray/triangle intersection.* In *ACM SIGGRAPH 2005 Courses,* SIGGRAPH '05, New York, NY, USA, 2005. ACM.

[9] Nedel, Luciana Porcher & Thalman, Daniel, *Real Time Muscle Deformations Using Mass-Spring Systems* Computer Graphics International, 1998. Proceedings, p. 156-165.

[10] L. Nilson *Real-time simulation of diaphragm displacement during physiological and mechanical ventilation*, 2013, Student Thesis, http://uu.diva-portal.org/smash/get/diva2:631804/FULLTEXT01.pdf

[11] McConville, J.F. and J.P. Kress, *Weaning patients from the ventilator.* New England Journal of Medicine, 2012. 367(23): p. 2233-9.

[12] P.F. Villard, W. Bourne, F. Bello, *Interactive Simulation of Diaphragm Motion Through Muscle and Rib Kinematics.* Recent Advances in the 3D Physiological Human Springer London (Ed.) p. 91-103 (2009)

[13] Visual Computing Lab ISTI-CNR. *Meshlab.* available: http://meshlab.sourceforge.net/